INTERNATIONAL JOURNAL OF INTEGRATED ENGINEERING
ISSN: 2229-838X e-ISSN: 2600-7916

IJIE

Vol. 17 No. 8 (2025) 272-284
https://publisher.uthm.edu.my/ojs/index.php/ijie

# Characterization of Bottom Ash from the Combustion of Palm Oil Empty Fruit Bunches (EFB)

**Amru Hamdi Fu'ad[1], Shahrin Hisham Amirnordin[1]*, Ahmad Jais Alimin[1], Shahrul Azmir Osman[1], Azian Hariri[1], Norasikin Mat Isa[1], Amir Khalid[1], Mohd Faizal Tukimon[1], Zulkifli Mohd Rosli[2], Mohammad Faizal Jabbar[3]**

[1] *Faculty of Mechanical and Manufacturing Engineering, Universiti Tun Hussein Onn Malaysia (UTHM), Parit Raja, Johor, 86400, MALAYSIA*

[2] *Faculty of Industrial and Manufacturing Technology and Engineering, Universiti Teknikal Malaysia Melaka, Hang Tuah Jaya, Melaka, 76100, MALAYSIA*

[3] *Classic Green Resources Sdn. Bhd., No. 18B, Jalan BK5A/2A, Bandar Kinrara, Puchong, Selangor, 47180, MALAYSIA*

*Corresponding Author: shahrin@uthm.edu.my
DOI: https://doi.org/10.30880/ijie.2025.17.08.023

**Article Info**

Received: 10 May 2025
Accepted: 29 November 2025
Available online: 31 December 2025

**Keywords**

Biomass combustion, bottom ash characterization, combustion analysis, Empty Fruit Bunch (EPB), pelletized biomass

**Abstract**

The palm oil industry generates large volumes of biomass waste, particularly Empty Fruit Bunches (EFB), which pose environmental disposal challenges but offer potential as a renewable energy source. This study focuses on the characterization and combustion analysis of bottom ash derived from pelletized EFB, with special attention to how combustion temperature affects ash quality at a fixed time duration. Pelletized EFB offers improved energy density and uniform combustion behavior compared to loose EFB. Combustion was conducted for 30 minutes at three different temperatures: 400°C, 600°C, and 800°C. The results showed that combustion temperature significantly influences ash yield and composition. Lower temperatures produced darker ash with higher residual carbon, while higher temperatures generated lighter ash with more fused and mineral-rich phases containing silicon, potassium, and calcium. XRD analysis confirmed a transition from simple crystalline phases at low temperatures to more complex silicate and glassy phases at higher temperatures, suggesting potential for construction-related applications. TGA revealed that major mass loss occurred between 200-375 °C due to decomposition of hemicellulose and cellulose, leaving about 33% inorganic residue forming the ash. Overall, this study highlights the critical role of combustion temperature in determining the physicochemical and mineralogical characteristics of EFB bottom ash and supports its potential for sustainable utilization within the palm oil industry.

## 1. Introduction

The palm oil industry is a significant contributor to Malaysia's economy and a major source of biomass waste, particularly in the form of Empty Fruit Bunches (EFB) [1 - 5]. These residues are often discarded or inefficiently managed, resulting in negative environmental impacts such as greenhouse gas emissions and landfill overuse. However, EFB holds high potential as a renewable biomass fuel due to its lignocellulosic content and abundant availability [6 - 11].

Combustion of EFB for energy generation presents a practical and scalable solution, and the use of pelletized EFB enhances its energy density, combustion efficiency, and ease of handling [12-17]. However, this process generates bottom ash, a by-product that, if not properly managed, may pose further environmental challenges [18-22]. An understanding of bottom ash characteristics is therefore essential to promote sustainable reuse and reduce disposal issues.

The composition and quality of bottom ash are greatly influenced by combustion parameters such as temperature and time. Previous research has primarily focused on combustion temperature as a variable due to its direct effect on ash morphology, chemical transformation, and thermal behavior. Higher temperatures are generally associated with more complete combustion, reduced unburned carbon, and improved crystalline structure in the ash, making it more suitable for reuse in industries such as construction and agriculture [6] [18].

This study investigates the effect of three combustion temperatures (400°C, 600°C, and 800°C) on bottom ash produced from EFB pellets over a constant combustion duration of 30 minutes. Through physical, chemical, and thermal characterization of the resulting ash, the research aims to identify optimal combustion conditions that yield ash suitable for secondary applications [23 - 24].

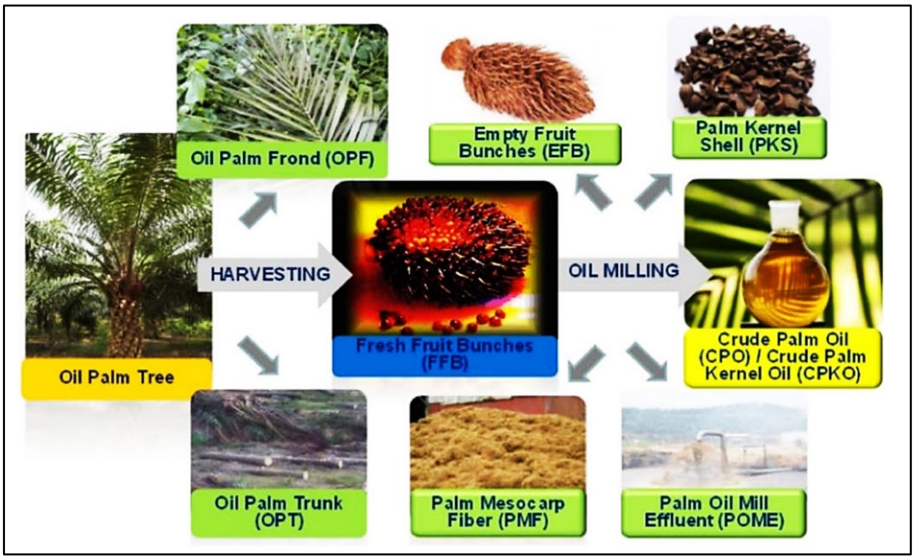


**Fig. 1** *Mainly from milling and harvesting oil palm [11]*

Ultimately, the findings of this study are expected to support circular economy practices by promoting the valorization of biomass waste into functional materials, reducing reliance on non-renewable resources, and contributing to more sustainable energy and waste management systems.

## 2. Methodology

This chapter presents a comprehensive methodology for investigating the characterization and combustion analysis of bottom ash derived from the combustion of palm oil Empty Fruit Bunches (EFB). The methodology is systematically designed to address the research objectives through a structured experimental approach that encompasses sample preparation, controlled combustion processes, and multi-dimensional analytical characterization techniques. The experimental framework adopts a rigorous scientific approach to ensure reproducible and reliable results that contribute to the understanding of EFB combustion behavior, and the subsequent properties of bottom ash produced under varying combustion conditions.

### 2.1 Sample Preparation

EFB dried to 15%, pulverized, and compacted into uniform cylindrical pallets using a palletizer. Fig. 2 shows the process of EFB pellet production. Each combustion experiment utilized 1kg of prepared EFB pallet samples, which represent an optimal quantity for achieving complete combustion while generating sufficient bottom ash for comprehensive characterization. During preparation, pallet EFB was ground and sieved to remove particles smaller than 250 microns using stainless-steel mesh size 69 microns. After that, the samples were prepared according to the experimental setup for each test. Before each experiment, the combustion chamber underwent thorough cleaning and preheating procedures to eliminate any residual materials from previous experiments and establish stable thermal conditions.

The loading procedure involved careful placement of the prepared EFB pallet samples to maximize surface area exposure to the combustion air while preventing sample agglomeration that could lead to incomplete combustion. The mesh platform design facilitated efficient ash separation, allowing bottom ash to settle at the chamber base while enabling proper air circulation throughout the fuel bed. Temperature monitoring was continuously maintained using multiple thermocouples positioned at different locations within the combustion zone to ensure uniform thermal conditions throughout the experimental duration.


**Fig. 2** *EFB pallet production procedure [3]*

## 2.2 Combustion Process

EFB pellets were combusted in a muffle furnace for 30 minutes. Combustion was carried out at three different temperatures: 400°C, 600°C, and 800°C. Fig. 3 shows the schematic diagram and actual combustion chamber for this experiment.

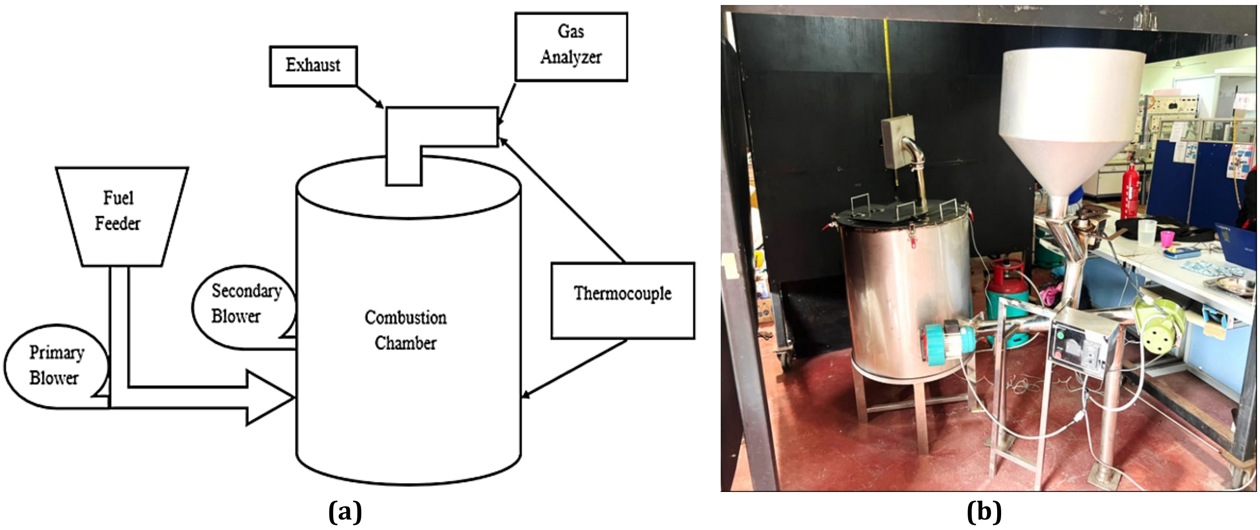


**Fig. 3** *(a) Schematic diagram of combustion chamber; (b) Actual combustion chamber*

## 2.3 Ash Collection and Storage

Bottom ash collection was performed immediately after the cooling process to minimize exposure to atmospheric moisture and prevent contamination. The collected ash samples were carefully separated from any unburned material through mechanical sieving to 70-micron sizes, ensuring the purity of the ash samples for subsequent characterization. Fig. 4 shows the sample collection after the sieving process.

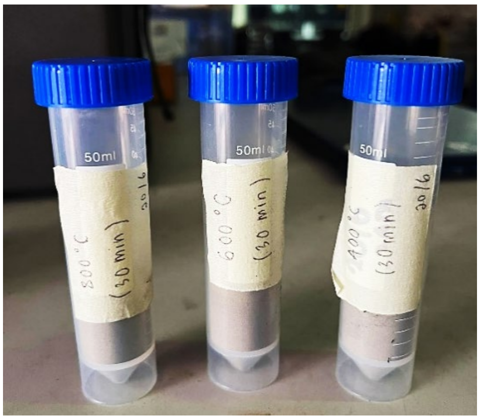


**Fig. 4** *Sample collection*

## 2.4 Analytical Techniques

In this study, several analytical techniques were employed to comprehensively characterize the bottom ash derived from the combustion of palm oil Empty Fruit Bunch (EFB), as listed in Table 1. Scanning Electron Microscopy (SEM) was used to observe the surface morphology of the ash, providing detailed information on particle shape and texture. The elemental composition of the sample was determined using Energy Dispersive X-ray Spectroscopy (EDX), which identifies key elements such as silicon (Si), potassium (K), calcium (Ca), and magnesium (Mg) commonly present in biomass ash. Meanwhile, X-ray Diffraction (XRD) analysis was conducted to investigate the crystal structure of the ash, distinguishing between amorphous and crystalline mineral phases that influence its reactivity and potential applications. Additionally, Thermogravimetric Analysis (TGA) was utilized to study the thermal decomposition behaviours of the bottom ash, revealing its degradation profile, mass loss characteristics, and overall thermal stability. Collectively, these techniques provided a comprehensive understanding of the physicochemical and structural properties of EFB bottom ash.

**Table 1** *Analytical techniques for biomass ash characterization*

| Technique | Purpose | Information provided |
|---|---|---|
| Scanning Electron Microscopy (SEM) | Surface morphology | Porosity, particle shape and texture |
| Energy Dispersive X-ray Spectroscopy (EDX) | Elemental composition | Key elements (Si, K, Ca, Mg) |
| X-ray Diffraction (XRD) | Crystal structure analysis | Amorphous vs crystalline mineral phases |
| Thermogravimetric analysis (TGA) | Thermal decomposition behaviour | Degradation profile, mass loss, thermal stability |

## 3. Results and Discussion

The study was conducted using a constant combustion duration of 30 minutes and three different temperatures: 400°C, 600°C, and 800°C. For each experiment, 1 kg of EFB pellets was combusted in a controlled laboratory reactor. The resulting bottom ash samples were then analyzed using Scanning Electron Microscopy coupled with Energy Dispersive X-ray Spectroscopy (SEM-EDX), X-ray Diffraction (XRD) and Thermogravimetric Analysis (TGA) to evaluate their morphological, elemental, and thermal characteristics. The main objective of this chapter is to report the observed differences in ash morphology, elemental composition, and thermal stability as a function of combustion temperature. The findings provide valuable insights into the combustion behavior of EFB pellets and the potential for bottom ash reuse or further processing.

## 3.1 Visual Observation and Ash Yield

After each combustion experiment, the bottom ash was collected and visually inspected. The appearance, color, and texture of the ash varied noticeably with combustion temperature. At a combustion temperature of 400°C, the bottom ash appeared dark grey to black in color, indicating the presence of unburned carbon and suggesting incomplete combustion at this relatively low temperature. When the temperature increased to 600°C, the ash colour lightened to grey and exhibited a finer, more powdery texture, reflecting a more complete combustion process with reduced carbon content, as shown in Fig. 5. At the highest temperature tested, 800°C, the ash was light grey to almost white. It displayed a more fused and granular appearance, implying significant mineral transformation and near-complete removal of organic matter during combustion.

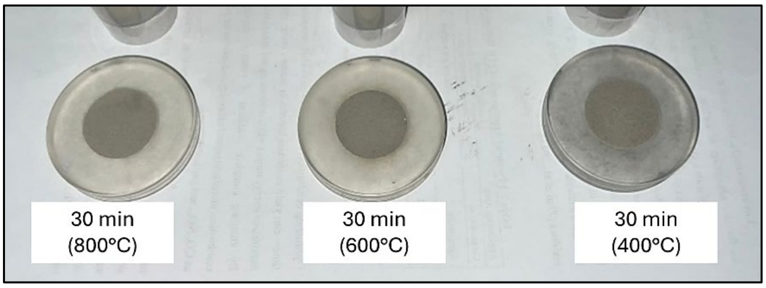


**Fig. 5** *Visual observation of EFB after combustion*

## 3.2 SEM Analysis

The surface morphology of the bottom ash derived from palm oil Empty Fruit Bunch (EFB) combustion was examined using Scanning Electron Microscopy (SEM) to evaluate the influence of temperature on particle structure and texture. SEM analysis provides detailed visual evidence of changes in particle size, shape, and surface characteristics as the combustion temperature increases. Through this method, agglomeration and degree of sintering have been observed, offering valuable insights into the thermal transformation and physical behavior of the ash. Understanding these morphological changes is essential for determining the suitability of EFB bottom ash for further utilization, such as in construction materials or environmental applications. Fig. 6 shows the SEM images of EFB combustion at 400°C at different magnifications.

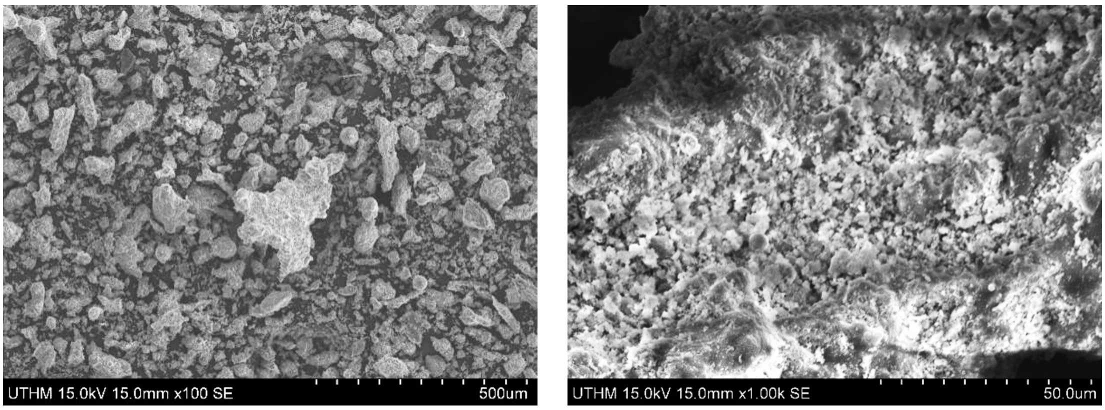


**(a)** **(b)**

**Fig. 6** *Magnifying SEM (a) 400°C x100; (b) 400°C x1000*

Based on Fig. 6, SEM observations of the bottom ash derived from EFB combustion at 400°C reveal that particles retained irregular and non-spherical shapes with porous, rough, and jagged surfaces. Many particles form loose agglomerates, possibly resulting from condensation of vapors onto cooler particles or mechanical clustering during cooling, and traces of unburned organic matter or fibrous residues are still evident. The porous structure likely imparts a moderate specific surface area, enabling better penetration of reactive agents but also introducing structural weaknesses or sites liable to ingress of unwanted species. These morphological traits are consistent with the behavior of biomass ashes reported in the literature. For instance, non-wood biomass ashes often display angular, aggregated particles with fine fragments adhering to larger ones, and variable morphology among biomass ashes has been correlated with differences in reactivity and suitability for applications such as alkali-activation or adsorption processes [11], [12].

At 600 °C (Fig. 7), the ash particles show a transition toward more fragmented and less fibrous morphology. The surfaces appear smoother than at 400 °C, and edges become more defined, indicating that thermal decomposition has progressed further and some degree of coalescence or sintering has occurred. The reduction in fibrous remnants suggests more complete burnout of organic matter, while the smoother surfaces and sharper particle boundaries point toward partial densification of the mineral phases. At 800 °C (Fig. 8), the ash particles appear notably more compact, with clear evidence of partial melting, fusion, or vitrification in localized zones. Surfaces may show glassy or glazed patches, and the internal porosity is reduced, giving a denser, less porous structure overall. Some particles may have partially fused, indicating that at this higher temperature, mineral phases began to soften or re-crystallize and bond at contact points, reducing free voids and increasing structural rigidity.

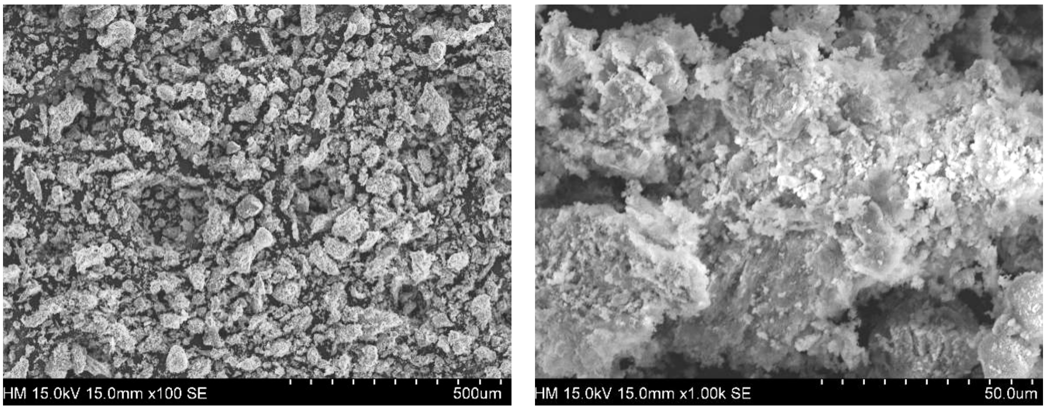


(a) (b)

**Fig. 7** *Magnifying SEM (a) 600°C x 100; (b) 600°C x 1000*

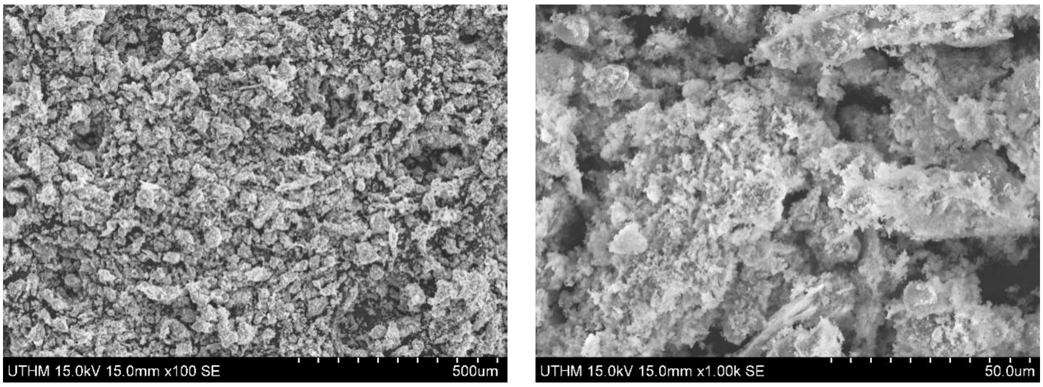


(a) (b)

**Fig. 8** *Magnifying SEM (a) 800°C x 100; (b) 00°C x 1000*

## 3.3 Elemental Composition

The elemental composition of the bottom ash samples was analyzed using Energy Dispersive X-ray Spectroscopy (EDX) coupled with Scanning Electron Microscopy (SEM). The results reveal significant variations in the elemental distribution as a function of combustion temperature, reflecting the chemical transformations occurring during the thermal degradation of EFB pellets. EDX spectra at all temperatures showed the presence of major inorganic elements such as silicon (Si), potassium (K), calcium (Ca), magnesium (Mg), and trace amounts of iron (Fe) and aluminum (Al). These elements are typical constituents of biomass ash and originate from the inherent mineral content of the original EFB material, as well as from the combustion process itself.

The carbon content is notably high at the lowest combustion temperature of 400°C, indicating incomplete combustion and the presence of residual unburned organic matter. As the temperature increases to 600°C and 800°C, the carbon content decreases substantially, demonstrating more complete oxidation of organic compounds and enhanced combustion efficiency. This carbon reduction is consistent with the visual observation of ash color lightening, and the transition from porous to more fused ash morphology [13].

Silicon, primarily present as silica ($SiO_2$), shows an increasing trend with temperature. This is attributed to the concentration of inorganic minerals as organic matter volatilizes and combusts away. Silicon plays a crucial role in determining the physical properties of ash, including its melting behavior and potential for forming crystalline silicate phases, which are confirmed by XRD analysis.

Potassium and calcium are among the most abundant alkali and alkaline earth metals detected in the ash. Their concentrations increase with combustion temperature due to the volatilization of other elements and the relative enrichment of these minerals in the residual ash. Potassium, in particular, is known to influence slagging and fouling tendencies in combustion systems due to its low-melting-point compounds. Calcium contributes to ash stability and can form compounds such as calcium silicates and carbonates, which affect the ash's structural properties. Magnesium, iron, and aluminum are present in smaller but significant amounts. These elements contribute to the formation of various mineral phases and influence the chemical reactivity and thermal stability of the ash. For instance, iron oxides can act as catalysts during combustion, while aluminum oxides contribute to ash hardness and durability.

Overall, the elemental composition analysis highlights the dynamic in ash chemistry with increasing combustion temperature (Table 2). The enrichment of mineral elements and depletion of carbon reflect the progressive conversion of biomass into inorganic residues. These chemical changes directly impact the physical behavior, thermal stability, and potential applications of bottom ash, such as its suitability for use in construction or as a soil amendment.

**Table 2** *Summary of elemental composition of ash at different temperatures*

| Element | Temperature | | |
|---|---|---|---|
| | 400°C | 600°C | 800°C |
| C | 12.0 | 8.5 | 2.2 |
| O | 49.76 | 46.30 | 41.64 |
| Si | 10.84 | 13.83 | 15.52 |
| K | 18.05 | 20.57 | 24.96 |
| Ca | 6.06 | 4.81 | 6.70 |
| Mg | 3.80 | 2.13 | 3.84 |
| Fe | 2.24 | 3.23 | 2.72 |
| Al | 2.02 | 4.64 | 2.14 |

## 3.4 Thermogravimetric Analysis (TGA)

Thermogravimetric analysis (TGA) was conducted on raw Empty Fruit Bunch (EFB) pellets to investigate their thermal decomposition behavior under controlled heating. The TGA curve, along with its derivative (DTG) and heat flow data, provides insights into the stages of mass loss and the thermal stability of the raw biomass prior to combustion.

The TGA curve for raw EFB pellets (Fig. 9) reveals several distinct stages of mass loss as the temperature increases from room temperature to 1000°C. The initial mass loss, occurring below 200°C, is relatively minor and is primarily attributed to the evaporation of moisture and the release of physically bound water from the EFB pellets. The most significant mass loss takes place during the main decomposition stage, between approximately 204°C (onset) and 373°C (offset), as indicated by the DTG peak centered at 319°C. This stage corresponds to the rapid decomposition of hemicellulose and cellulose, which are the main organic components of EFB.

Furthermore, the mass loss in this region is substantial, with a reaction step at 319°C resulting in a 47.1% reduction in mass, consistent with the thermal degradation of polysaccharides that typically decompose within this temperature range. Following this, a secondary decomposition phase occurs from 375°C to about 500°C, during which further mass loss brings the total mass change to 59.4% (Table 3). This phase is associated with the breakdown of more thermally stable components, such as lignin, and the continued volatilization of organic matter. Beyond 500°C, the rate of mass loss slows considerably, with only minor changes observed up to 1000°C. The final residual mass at 1000°C is approximately 33% of the initial sample mass, indicating that about 67% of the original mass has been lost as volatiles and gases. The remaining material is primarily composed of inorganic minerals and ash-forming constituents, reflecting the mineral residue left after complete thermal decomposition of the organic matter in the EFB pellets.

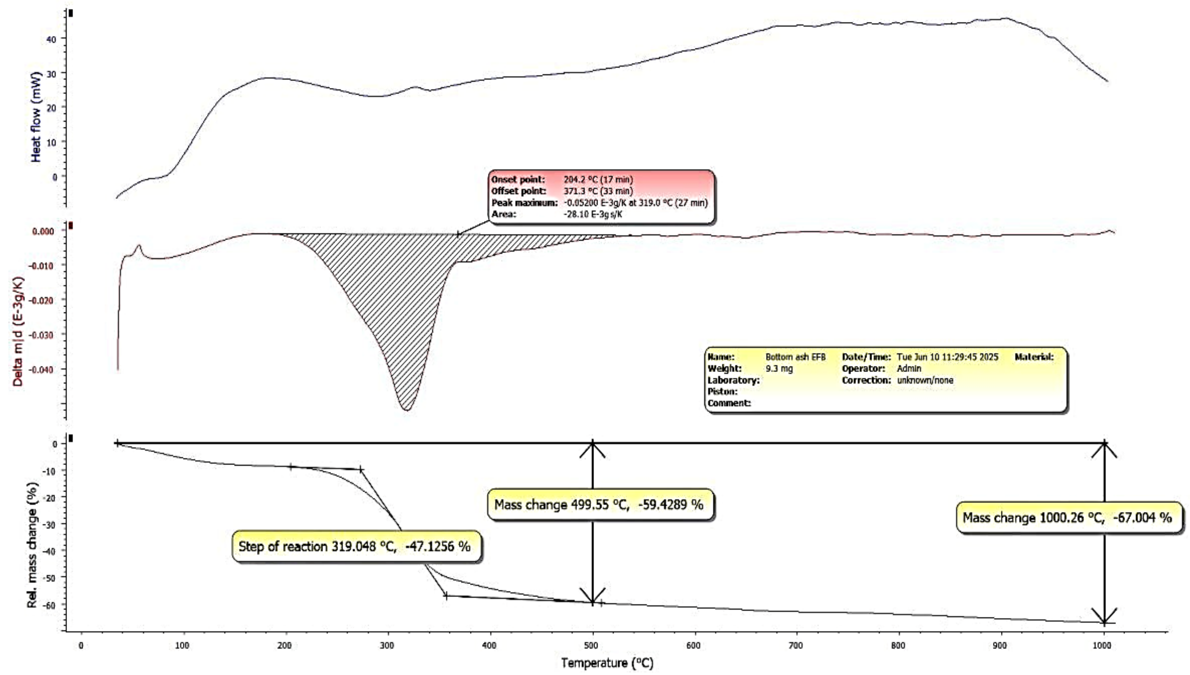


**Fig. 9** *TGA and DTG curves of raw EFB pellets*

**Table 3** *Summary of TGA data testing*

| Temperature (°C) | Mass change (%) | Stage description |
|---|---|---|
| ~100 | -5% | Moisture evaporation |
| 204–373 | -47.1% | Rapid decomposition of hemicellulose/cellulose |
| Up to 500 | -59.4% | Continued lignin degradation, further volatiles |

## 3.5 X-ray Diffraction (XRD) Analysis

An X-ray Diffraction (XRD) analysis was conducted to identify the crystalline phases present in the bottom ash samples produced at 400°C, 600°C, and 800°C. The results indicate a clear transformation of mineral phases and crystalline structures depending on the combustion temperature, which reflects the extent of thermal decomposition and mineral restructuring in the ash. According to Fig. 10, at 400°C, the bottom ash primarily consisted of Chlorocalcite ($KCaCl_3$) with a relative intensity (Y%) of 90.45%, along with Bartonite ($K_3Fe_{10}S_{14}$) at 69.21%. Other minor compounds such as Sylvite (KCl), Potassium Sulfide ($K_2S_3$), and Troilite (FeS) were also identified. The relatively moderate intensities and peak broadness at this temperature indicate incomplete combustion and limited crystalline development, as not enough thermal energy was supplied to fully convert the organic matrix into stable mineral forms.

At 600°C, as shown in Fig. 11, the XRD profile exhibited more defined and sharper peaks, indicating increased crystallinity. Chlorocalcite remained the dominant phase, with a significantly higher intensity of 129.60%, followed by Bartonite at 88.93%. The continued presence of Sylvite (64.90%) and Potassium Sulfide (43.65%) suggests more thorough mineral evolution. Troilite was still detectable but appeared less intense. These results align with earlier TGA and SEM findings, confirming that 600°C is the optimal combustion temperature at which sufficient thermal decomposition occurs without excessive sintering, resulting in balanced mineral formation and a stable ash structure.

Fig. 12 presents the XRD results at 800 °C, where the diffraction patterns exhibit clear signs of intense crystallization and mineral densification, as indicated by sharper and more symmetrical peaks. Similar high-temperature transformations have been reported in biomass ash studies, where increasing temperature promotes mineral ordering, recrystallization, and structural consolidation [14]. The emergence of a highly crystalline elemental sulfur phase may be attributed to sulfur volatilization followed by redeposition at elevated temperatures; a behavior commonly observed in biomass ash systems undergoing volatilization and condensation cycles. The persistence of K–Cl minerals such as chlorocalcite and sylvite is consistent with previous reports showing that alkali salts can remain stable or reform under high-temperature combustion conditions. Furthermore, the increased sharpness and symmetry of the diffraction peaks indicate enhanced mineral alignment, suggesting potential ash fusion or slagging, which aligns with earlier findings that higher crystallinity and reduced porosity can limit ash reactivity in reuse applications [15]. The summary of the XRD findings is tabulated in Table 4.

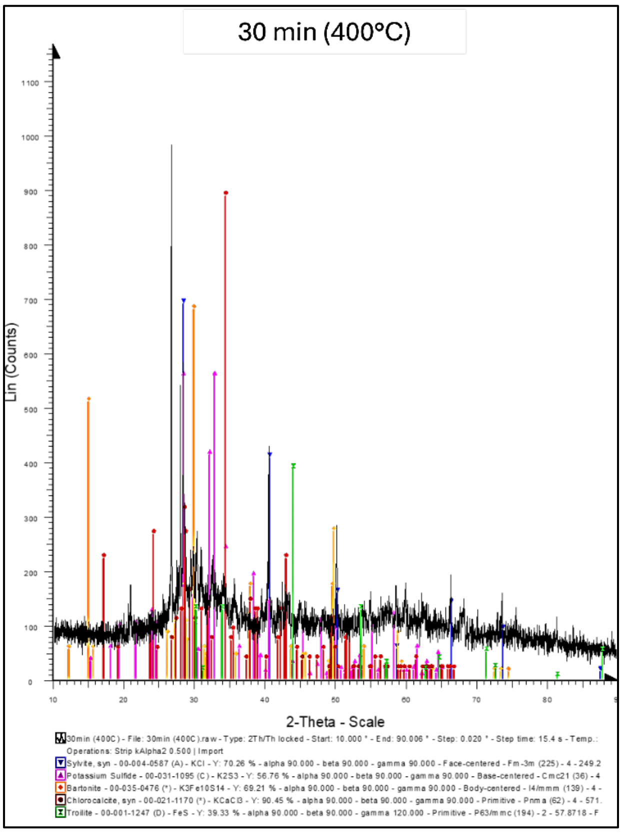


**Fig. 10** *XRD result for 400°C 30 minutes*

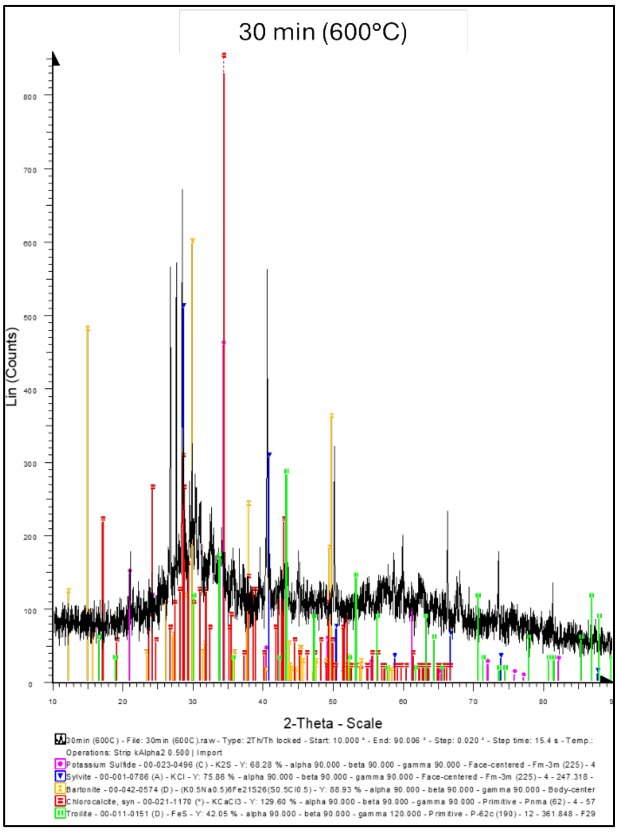


**Fig. 11** *XRD Result for 600°C 30 minutes*

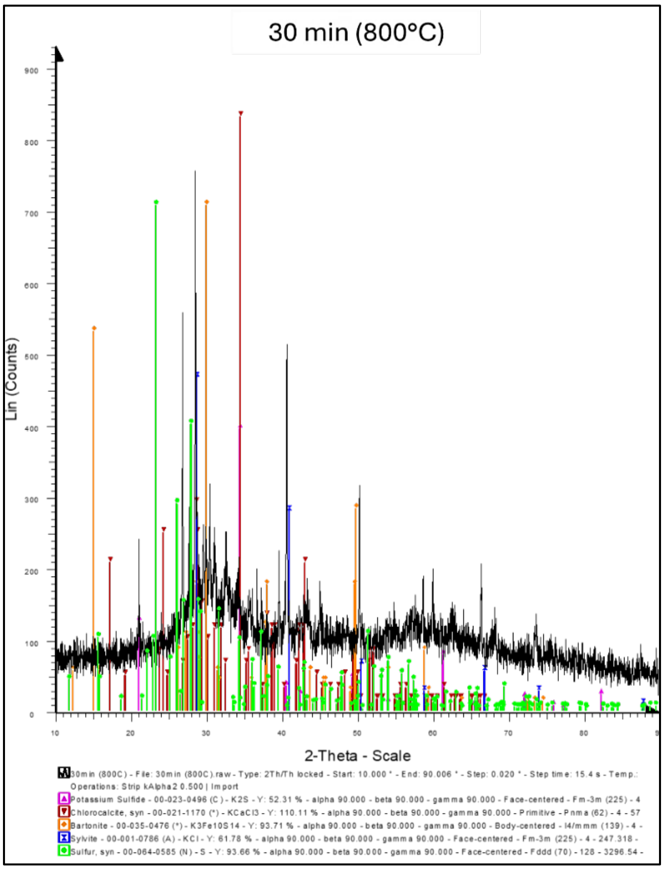


**Fig. 12** *XRD result for 800°C 30 minutes*

**Table 4** *Summary of XRD Results for Bottom Ash Samples Produced at 400°C, 600°C, and 800°C*

| Temperature (°C) | Major compound Identified | Chemical formula | Crystalline structure | Relative intensity (Y%) | Remarks |
|---|---|---|---|---|---|
| 400 | Chlorocalcite | $KCaCl_3$ | Orthorhombic | 90.45% | Primary phase, moderate crystallinity |
| | Bartonite | $K_3Fe_{10}S_{14}$ | Monoclinic | 69.21% | Sulfide compound, iron-rich |
| | Sylvite | KCl | Cubic | 56.70% | Common in alkali-rich biomass ash |
| | Potassium sulfide | $K_2S_3$ | Unknown | 40.31% | Minor phase |
| | Troilite | FeS | Hexagonal | 47.08% | Sulfur-bound iron |
| 600 | Chlorocalcite | $KCaCl_3$ | Orthorhombic | 129.60% | Dominant, highly crystalline |
| | Bartonite | $K_3Fe_{10}S_{14}$ | Monoclinic | 88.93% | More intense, stable phase |
| | Sylvite | KCl | Cubic | 64.90% | Stable at elevated temperature |
| | Potassium sulfide | $K_2S$ | Unknown | 43.65% | Trace presence remains |
| | Troilite | FeS | Hexagonal | 45.12% | Slight evolution from 400°C |
| 800 | Bartonite | $K_3Fe_{10}S_{14}$ | Monoclinic | 93.71% | Peak crystallinity, dominant phase |
| | Sulfur | S | Face-centered cubic | 93.66% | New peak, possibly from sulfur sublimation |
| | Chlorocalcite | $KCaCl_3$ | Orthorhombic | 89.30% | Still present, less intense than at 600°C |
| | Sylvite | KCl | Cubic | 62.55% | Retained from earlier phases |
| | Potassium sulfide | $K_2S$ | Unknown | 35.45% | Fused structure suspected |

Overall, the XRD results demonstrate that combustion temperature plays a vital role in determining the mineralogical composition and crystalline behavior of bottom ash. While 400°C resulted in underdeveloped ash with weak crystalline structure, 600°C yielded optimal phase formation with balanced properties. In contrast, 800°C enhanced crystalline intensity but introduced structural fusion, making the ash less suitable for pozzolanic or soil applications due to reduced surface activity. These insights are critical for selecting the appropriate combustion condition for bottom ash management and value-added reuse.

## 4. Conclusions

This study successfully derived and characterized bottom ash produced from the controlled combustion of palm oil empty fruit bunch (EFB) pellets at 400°C, 600°C, and 800°C. The systematic experiments confirmed that combustion temperature critically governs the physical, chemical, and mineralogical properties of the resulting ash. At lower temperatures, the ash exhibited darker coloration, higher residual carbon, and incomplete combustion, whereas higher temperatures produced lighter-coloured, more fused ash rich in inorganic constituents such as Si, K, and Ca. The SEM analysis revealed a progressive transformation from porous, fibrous particles to denser, sintered structures, while XRD confirmed the transition from simple crystalline phases at 400 °C to complex silicate and glassy phases at 800°C. TGA further validated that major mass losses occurred during the decomposition of hemicellulose and cellulose, leaving approximately one-third inorganic residue as bottom ash. Overall, the successful derivation and detailed characterization of EFB bottom ash demonstrate that combustion temperature plays a decisive role in determining ash formation, structure, and potential reuse. These outcomes not only strengthen the understanding of biomass ash behaviour but also highlight the potential of EFB bottom ash as a value-added by-product for sustainable material applications and waste minimization in the palm oil industry.

## Acknowledgement

This research was supported by the Ministry of Higher Education (MOHE) through the Industrial Matching Research Grant Scheme (IMaP/2/2024/TK08/UTHM//1). We also want to thank to the Classic Green Resources Sdn. Bhd. for sponsoring and providing data collection for this work.

## Conflict of Interest

The authors declare that there is no conflict of interest regarding the publication of the paper.

## Author Contribution

*The authors confirm contribution to the paper as follows:* ***study conception and design:*** *Amru Hamdi Fu'ad;* ***data collection:*** *Amru Hamdi Fu'ad;* ***analysis and interpretation of results:*** *Shahrin Hisham Amirnordin, Zulkifli Mohd Rosli, Najib Nasir;* ***draft manuscript preparation:*** *Amru Hamdi Fu'ad, Shahrin Hisham Amirnordin, Mohd Faizal Mohideen Batcha, Norasikin Mat Isa, Hamimah Abd Rahman, Amir Khalid, Mohd Faizal Tukimon. All authors reviewed the results and approved the final version of the manuscript.*

## References

[1] T. P. Xiong, A. Kasani, S. H. Amirnordin, M. Faizal, and M. Batcha, "Experimental Investigation of Flame Stability and Temperature Profiles in an LPG-Fuelled Combustion System for Industrial Hot Air Generation," J. Adv. Res. Des., vol. 1, no. 1, pp. 55–68, 2026, [Online]. Available: https://akademiabaru.com/submit/index.php/ard.

[2] Chang, S. H. (2014). An overview of empty fruit bunch from oil palm as feedstock for bio-oil production. *Biomass and Bioenergy*, *62*, 174–181. https://doi.org/10.1016/J.BIOMBIOE.2014.01.002

[3] *Growing media-palm peat| palm short fiber| coco peat- MacFiber*. (n.d.). Retrieved June 13, 2025, from https://www.macbaler.com/balers/growing-media-palm-peat-palm-short-fiber/

[4] James Rubinsin, N., Daud, W. R. W., Kamarudin, S. K., Masdar, M. S., Rosli, M. I., Samsatli, S., Tapia, J. F., Wan Ab Karim Ghani, W. A., & Lim, K. L. (2020). Optimization of oil palm empty fruit bunches value chain in Peninsular Malaysia. *Food and Bioproducts Processing*, *119*, 179–194. https://doi.org/10.1016/J.FBP.2019.11.006

[5] Jafri, Jimat, Azmin, Sulaiman, and Nor, "The potential of biomass waste in Malaysian palm oil industry : A case study of Boustead Plantation Berhad," Mater. Sci. Eng., vol. 1192, no. 012028, pp. 0–10, 2021, doi: 10.1088/1757-899X/1192/1/012028.

[6] Sepúlveda Olea, F. E., Burke, I. T., Mohammad, A., & Stewart, D. I. (2024). Reuse potential of municipal solid waste incinerator bottom ash as secondary aggregate: Material characteristics, persistent organic pollutant content and effects of pH and selected environmental lixiviants on leaching behaviour. *Waste Management*, *187*, 262–274. https://doi.org/10.1016/J.WASMAN.2024.07.026

[7] Sumathi, S., Chai, S. P., & Mohamed, A. R. (2008b). Utilization of oil palm as a source of renewable energy in Malaysia. *Renewable and Sustainable Energy Reviews*, *12*(9), 2404–2421. https://doi.org/10.1016/J.RSER.2007.06.006

[8] T. Hardianto, "Upgrading process of palm empty fruit bunches as alternative solid fuel : a review," Oxford, vol. 7, no. 6, pp. 1173–1188, 2023. https://doi.org/10.1093/ce/zkad059

[9] R. Dolah, R. Karnik, and H. Hamdan, "A Comprehensive Review on Biofuels from Oil Palm Empty Bunch ( EFB ): Current Status , Potential , Barriers and Way Forward," Sustainability, vol. 13, no. 10210, pp. 1–29, 2021, doi: https://doi.org/10.3390/su131810210.

[10] A. Irawan, "Potential and Opportunity of Co-Firing Power Plant in Indonesia Through Torrefaction of Empty Fruit Bunch (EFB) - A Review," World Chem. Eng. J., vol. 5, no. 1, pp. 25–32, 2021.

[11] Amirnordin, S. H., Batcha, M. F. M., Kasani, A., Jalal, M. A., Khalid, A., Mustafa, K. F., & Zainudin, K. E. A. (2023). Combustion Characteristic of Empty Fruit Bunch From Palm Oil Mill Waste. Journal of Industry, Engineering and Innovation, 5(2), 14-17.

[12] Nick, Z., & Lagerkvist, A. (2011). Phosphorus recovery from the biomass ash: A review. *Renewable and Sustainable Energy Reviews*, *15*(8), 3588–3602. https://doi.org/10.1016/j.rser.2011.05.016

[13] Batcha, M. F. M., Othaman, M. F., Sabudin, S., Mohammed, A. N., Abdullah, M. K., & Mas Fawzi, M. A. (2020). Combustion and emission of pelletized empty fruit bunch and oil palm shell in a swirling fluidized bed combustor. Biomass Conversion and Biorefinery, 10(4), 755–763. https://doi.org/10.1007/s13399-020-00903-x.

[14] M. Sukhairi et al., "Impact of pelletisation on torrefied oil palm empty fruit bunch biochar," Web Conf., vol. 05014, 2024. https://doi.org/10.1051/bioconf/202413105014

[15] M. M. Mustafa, M. Z. Muhamad, and M. H. Jalil, "Oil Palm Empty Fruit Bunch ( EFB ) Pellet and Rice Husk Pellet Biomass Fuel in Malaysia : A Comparative Investigation of Moisture , Dry Ash , and Oil Content," Int. J. Acad. Res., vol. 13, no. 11, pp. 1151–1170, 2023, doi: 10.6007/IJARBSS/v13-i11/19433.

[16] N. Aprianti, M. Faizal, M. Said, and S. Nasir, "Valorization of Palm Empty Fruit Bunch Waste for Syngas Production Through Gasification," J. Ecol. Eng., vol. 21, no. 7, pp. 17–26, 2020. https://doi.org/10.12911/22998993/125461

[17] A. Z. Ramli, S. Sabudin, M. Faizal, and M. Batcha, "Analysis of Tar Properties Produced During Co-Gasification of Empty Fruit Bunch Pellet and Oil Palm Shell," Int. J. Integr. Eng., vol. 3, pp. 52–59, 2020. https://doi.org/10.30880/ijie.2019.11.10.007

[18] Umar, M. S., Jennings, P., & Urmee, T. (2013). Strengthening the palm oil biomass Renewable Energy industry in Malaysia. *Renewable Energy*, *60*, 107–115. https://doi.org/10.1016/J.RENENE.2013.04.010

[19] Eliche-Quesada, D., López, M. J., & Jurado, M. (2021). Biomass bottom ash waste and by-products of the combustion process of a mix of pine-olive pruning in power plants. Resources, Conservation & Recycling, 167, 105464. https://doi.org/10.1016/j.resconrec.2021.105464

[20] Pertile, E., Dvorský, T., Václavík, V., Šimáčková, B., & Balcařík, L. (2024). Utilization of Bottom Ash from Biomass Combustion in a Thermal Power Plant to Remove Cadmium from the Aqueous Matrix. Molecules, 29(23), 5727. https://doi.org/10.3390/molecules29235727

[21] Kuswa, F. M., Prida Putra, H., Prabowo, Darmawan, A., Aziz, M., & Hariana, H. (2023). Investigation of the combustion and ash deposition characteristics of oil palm waste biomasses. Biomass Conversion and Biorefinery, 14, 24375-24395. https://doi.org/10.1007/s13399-023-04418-z

[22] Tans Ming, (2022). Use of Palm Oil Boiler Bottom Ash as Replacement Material in Lightweight Aggregate Concrete. PEAT (Periodical of Engineering and Applied Technology, UTHM). https://publisher.uthm.edu.my/periodicals/index.php/peat/article/view/6240

[23] Usman Jamo, H. (2015). Characterization Of A Treated Palm Oil Fuel Ash. *Science World Journal*, *10*(1). www.scienceworldjournal.org

[24] F. Matalkah, P. Soroushian, S. Ul Abideen, and A. Peyvandi, "Use of non-wood biomass combustion ash in development of alkali-activated concrete," Constr. Build. Mater., vol. 121, no. June, pp. 491–500, 2016, doi: 10.1016/j.conbuildmat.2016.06.023.

[25] O. J. Olatoyan, M. A. Kareem, A. U. Adebanjo, S. O. A. Olawale, and K. T. Alao, "Potential use of biomass ash as a sustainable alternative for fly ash in concrete production: A review," Hybrid Adv., vol. 4, no. June, 2023, doi: 10.1016/j.hybadv.2023.100076.

[26] Yuan, Y., Kang, R., & Ott, A. (2023). New insights into the synergistic effect on condensable vapours and ash particle growth in coal/pulverised fuel combustion. Aerosol and Air Quality Research, 23(6), oa-0145. https://aaqr.org/articles/aaqr-23-06-oa-0145

[27] Nabu Bakar, A. K., Hashim, N., & Mohd, Z. (2018). Improved process for the production of low-ash empty fruit bunches (EFB) pellets. Malaysian Palm Oil Board. https://palmoilis.mpob.gov.my/publications/TOT/TT577-Nasrin.pdf

[28] Mustafa, M. M. (2020). Oil palm empty fruit bunch (EFB) pellet and rice husk pellet biomass fuel in Malaysia: A comparative investigation of moisture, dry, ash and oil content. Human Resource Management Academic Research Society (HRMARS). doi: 10.6007/IJARBSS/v13-i11/19433.

[29] IHI Corporation. (2023). Sustainable Power Generation through Local Production and Consumption of EFB Pellets. Vol. 56, No. 2. https://www.ihi.co.jp/en/technology/techinfo/contents_no/__icsFiles/afieldfile/2023/11/24/Vol56No2_02.pdf

[30] Brunerová, A., Müller, M., Šleger, V., Ambarita, H., & Valášek, P. (2018). Bio-Pellet Fuel from Oil Palm Empty Fruit Bunches (EFB): Using European Standards for Quality Testing. Sustainability, 10(12), 4443. https://doi.org/10.3390/su10124443

[31] Ramli, A. Z., Sabudin, S., Mohideen Batcha, M. F., & Waehahyee, M. (2025). Analysis of tar properties produced during co-gasification of empty fruit bunch pellet and oil palm shell. International Journal of Energy Science. https://doi.org/10.30880/ijie.2019.11.10.007

[32] Liu, W., Wang, X., Zhao, B., Lu, J. (2023). New Insights into the Synergistic Effect on Condensable Particulate Matter Based on the Formation, Characteristics and Removal. Aerosol Air Qual. Res. 23, 230145. https://doi.org/10.4209/aaqr.230145

[33] Yamada, H., Yamauchi, H. & Kurimoto, Y. Color analysis of combustion ashes of seawater-soaked wood: estimation of salt concentration. *J Mater Cycles Waste Manag* 16, 576–582 (2014). https://doi.org/10.1038/s41560-019-0336-z

[34] Nelson, E. S., Iyuke, S., Daramola, M. O., & Okewale, A. (2023). Extraction and Characterization of Silica from Empty Palm Fruit Bunch (EPFB) Ash. Processes, 11(6), 1684. https://doi.org/10.3390/pr11061684

[35] Kuswa, F. M., Prida Putra, H., Prabowo, Prabowo, Darmawan, A., Aziz, M., & Hariana, H. (2024). Investigation of the combustion and ash deposition characteristics of oil palm waste biomasses. Biomass Conversion and Biorefinery, 14, 24375–24395. https://doi.org/10.1007/s13399-023-04418-z

[36] Erdiwansyah, Asri Gani, Hera Desvita, Mahidin, Vera Viena, Rizalman Mamat, Ratnaningsih Eko Sardjono (2024). Analysis study and experiments SEM-EDS of particles and porosity of empty fruit bunches, Case Studies in Chemical and Environmental Engineering, 9, 100773. https://doi.org/10.1016/j.cscee.2024.100773.

[37] Kolajo T.E., Ewemoje O.E. and Adefowope G. (2024) Physico-chemical Assays of Oil Palm (Elais guineesis) empty fruit bunch fractions for biosynthesis, J. Mater. Environ. Sci., 15(3), 386-396. http://www.jmaterenvironsci.com

[38] Li, J., Long, X., Zhu, H., Liu, Z., Lu, X., & Zhang, D. (2023). Investigation into the fusibility of biomass ashes and their mineral phase transformations at elevated temperatures by using the HT-XRD technique. Biomass and Bioenergy, 173, Article 106812. https://doi.org/10.1016/j.biombioe.2023.106812

[39] Maj, I., Niesporek, K., Płaza, P., Maier, J., & Łój, P. (2025). Biomass Ash: A Review of Chemical Compositions and Management Trends. Sustainability, 17(11), 4925. https://doi.org/10.3390/su17114925

[40] M. Reinmöller *et al.*, “Formation and transformation of mineral phases in biomass ashes and evaluation of the feedstocks for application in high-temperature processes,” *Renew. Energy*, vol. 210, no. September 2022, pp. 627–639, 2023, doi: 10.1016/j.renene.2023.04.072.

[41] S. V. Vassilev, C. G. Vassileva, and N. L. Petrova, “Mineral Carbonation of Biomass Ashes in Relation to Their CO2Capture and Storage Potential,” *ACS Omega*, vol. 6, no. 22, pp. 14598–14611, 2021, doi: 10.1021/acsomega.1c01730.

[42] Soprych, P., & Czerski, G. (2025). The Use of Biomass Ash as a Catalyst in the Gasification Process—A Review. Energies, 18(21), 5653. https://doi.org/10.3390/en18215653